

Immunotherapy and prognosis of non-small cell lung carcinoma by monomethoxy polyethylene glycol-hyaluronic acid-platinum combined with immune CT4+ and CT8+ detection

Xubin Ren^{1#}, Tong Luo^{2#}, Hailong Ma³, Meili Zhou³, Shufang Yu^{4*}

¹ Department of Respiratory and Critical Care Medicine, Chengdu First People's Hospital, Chengdu, 610095, Sichuan, China

² Department of Pediatrics, Chengdu BOE Hospital, Chengdu, 610200, Sichuan, China

³ Emergency Center, Affiliated Qingdao Central Hospital, Qingdao University, Qingdao, 266042, Shandong, China

⁴ Zhejiang Pharmaceutical College, Fenghua District, Ningbo, 315100, Zhejiang, China

[#]These authors contributed equally to this work

ARTICLE INFO

Original paper

Article history:

Received: December 19, 2022

Accepted: March 09, 2022

Published: June 30, 2022

Keywords:

mPEG-HA-Pt; CT4+; CT8+;
Non-small cell lung carcinoma.

ABSTRACT

To investigate the changes in CT4+ and CT8+ lymphocyte subpopulations of patients with non-small cell lung carcinoma (NSCLC) by monomethoxy polyethylene glycol-hyaluronic acid-platinum (mPEG-HA-Pt) and the correlation between efficacy evaluation and the changes in T-lymphocyte subpopulation, 76 NSCLC patients treated at oncology department of Chengdu First People's Hospital were selected and randomly divided into the treatment group and the control group (38 cases in each). mPEG-HA-Pt was used for the treatment of the included patients in the research. The patients in the control group were performed with traditional chemotherapy for 2 treatment courses. The changes in the T-lymphocyte subpopulation before and after the treatment were detected and the therapeutic effects on the patients in the two groups were compared. The particle size of mPEG-HA-Pt ranged between 78nm and 100nm with an average of 84.6±7.5nm. After that, a transmission electron microscope (TEM) was used to observe the spheres with uniform size. The drug loading capacity and entrapped efficiency of mPEG-HA-Pt were 18.7% and 87.4%, respectively. After the treatment for NSCLC patients by nanomicelle, cellular immune functions were all improved. In particular, cellular immune functions of the patients with good efficacy evaluation were improved more apparently.

Doi: <http://dx.doi.org/10.14715/cmb/2022.68.6.27>

Copyright: © 2022 by the C.M.B. Association. All rights reserved.

Introduction

Lung carcinoma is a malignant tumor that seriously threatens human health and life. About 85% of lung carcinoma are non-small cell lung carcinoma (NSCLC). In 2022, the latest *National Cancer Report* released by National Cancer Center shows that the number of new patients with lung carcinoma in China is around 830,000 every year. NSCLC is the malignant tumor with the highest incidence and fatality (1,2). The risk factors for the incidence of NSCLC include smoking, alcohol consumption, environmental occupation, and genetic factors (3). At present, the main clinical treatment methods for NSCLC include chemoradiotherapy, complete resection of lung carcinoma primary focus, and lymph node metastasis, all of which are aimed at clinical cures.

T lymphocyte subpopulation level plays an important role in anti-tumor immune monitoring. The changes in T-lymphocyte subpopulation levels during NSCLC clinical staging, before and after NSCLC surgery, and before and after chemotherapy are reported in many studies (4-6). T-cell is a kind of immunocyte originating mainly from pluripotent stem cells (PSC) in bone marrow (from the yolk sac and liver during the embryonic stage). It mainly gets

involved in the cellular immune response. According to the types of a cluster of differentiation (CD) on the cell surface, the T-cell is divided into two subpopulations, including CD4+ and CD8+ (7,8). CD4+ mainly assists in the expression of T (Th) cells, which is a useful marker for the inhibition and assistance of the induction of subpopulations by cells in the identification of the T-lymphocyte subpopulation (9). CD8+ molecule is a kind of transmembrane glycoprotein that consists mainly of α and β polypeptide chains. The molecular weight of chain α is 34kDa and that of chain β is 30kDa. The two chains are linked by a disulfide bond at connecting peptides. Each polypeptide chain includes 1 IgV-like domain, connecting peptide, a transmembrane domain, and cytoplasmic domain (10).

The local drug delivery system refers to the treatment method for the direct delivery of drugs to tumor cells for taking effect. The system possesses the advantages of a high concentration of local drugs, high bioavailability, and quick body adaptability (11). Polyethylene glycol (PEG) shows strong hydrophilicity and is widely applied in the hydrophilic block of nanomicelle to accelerate the dissolution of platinum (Pt) drugs by micelle. As a kind of naturally degradable polymer material, hyaluronic acid (HA) can deliver Pt drugs into tumor tissues as a drug carrier

* Corresponding author. Email: yushufang2022@yandex.com

(12-14).

A targeting nanomicellar system (monomethoxy polyethylene glycol-hyaluronic acid-platinum (mPEG-HA-Pt)) formed by HA and platinum(II) chloride (DACHPt) modified by mPEG was designed and used in the research. Long circulation in the body was realized by the enhancement of the osmotic retention effect within the system. As a result, the high-level concentration of drugs at the lesion sites of NSCLC patients was improved and the toxic and side reactions to normal cell tissues were reduced.

Materials and Methods

Research objects

76 NSCLC patients treated at the Oncology Department of Chengdu First People's Hospital between May 2019 and May 2022 were selected, including 42 male patients and 34 female patients aged between 55 and 79. Their average age was 65.42 ± 8.64 . They were randomly divided into the treatment group and the control group (38 cases in each). According to Tumor Node Metastasis (TNM) staging released by Union for International Cancer Control (UICC), there were 31 cases with levels I and II and 45 cases with levels III and IV. The implementation of this research had been approved by Chengdu First People's Hospital Medical Ethics Committee. Besides, all patients and their family members had known about the research and signed informed consent forms.

Patients were included in the research based on the following inclusion criteria.

A. Patients diagnosed with NSCLC by pathological examination

B. Patients without infection history and the use of glucocorticoid or immunosuppressant drugs 1 month before the experiment

C. Patients without a history of immune diseases or family history (such as systemic lupus erythematosus and rheumatic osteoarthritis)

D. Patients with expected survival over 4 months and without contraindications of Pt drugs

Patients were excluded from the research based on the following exclusion criteria.

A. Patients who took glucocorticoid or immunosuppressant drugs 1 month before the experiment

B. Patients with complicated severe heart, liver, kidney, and other major diseases

C. Patients with complicated autoimmune diseases

Treatment methods

Based on Clinical Practice Guidelines in Oncology released by National Comprehensive Cancer Network (NCCN), the chemotherapy plan for NSCLC patients in the treatment group was formulated. A targeting nanomicellar system (mPEG-HA-Pt) was used for the treatment for 4 courses. The patients in the control group were performed with a traditional chemotherapy approach. Peripheral blood of the patients in the two groups was extracted to detect T-lymphocyte subpopulation levels and the changes in T-lymphocyte subpopulations before and after the treatment 20 days before and after the first immunotherapy. During each chemotherapy, the efficacy of chemotherapy was evaluated once every 2 courses and the therapeutic effects on the patients in the two groups were compared.

Efficacy evaluation indexes

According to RECIST 1.0 evaluation criteria (15), the evaluation of target lesions was divided into the following types.

A. Progressive disease (PD)

PD referred to the sum of long diameters of baseline lesions increased by 20% or more

B. Partial response (PR)

PR referred to the sum of long diameters of baseline lesions reduced by 30% or more

C. Stable disease (SD)

SD referred to the sum of long diameters of baseline lesions decreased less than PR or increased less than PD

D. Complete response (CR)

CR referred to the disappearance of all target lesions

The calculation methods for effective rate and stability rate were shown in equations 1 and 2 below.

$$RR = \frac{PR + CR}{PD + PR + SD + CR} \times 100\% \quad [1]$$

$$CBR = \frac{PR + SD + CR}{PD + PR + SD + CR} \times 100\% \quad [2]$$

Main reagents and instruments

The main experimental reagents included Tritest CD-4FITC /CD8PE /CD3PerCP reagent, 10×disposable hemolysin (Becton, Dickinson and Company (BD), U.S.), 1-ethyl-3-(3-dimethylaminopropyl)-carbodiimide (EDC, Sigma-Aldrich Company, U.S.), N-hydroxysuccinimide (NHS, Sigma-Aldrich Company, U.S.), DACHPt (Sigma-Aldrich Company, U.S.), HA (Lifecore Company, U.S.), and methoxypolyethylene glycols (mPEG-NH₂, Xi'an Kaixin Biotechnology Co., Ltd.)

The main experimental instruments included FACSCalibur flow cytometer (FCM, BD Company, U.S.), MercuryPlus 400 nuclear magnetic resonance spectrometer (Varian Company, U.S.), Zetasizer Nano ZS90 nano-particle potentiometer (Malvern Company, U.K.), Delta 1-24 LSC freezing dry machine (Christ Company, Germany), Fourier transform infrared spectrometer (FTIR, Nicolet Instrument Company, U.S.), and nuclear magnetic resonance spectrometer (Bruker 500, Bruker Company, Switzerland).

Detection of T-lymphocyte subpopulations

2mL peripheral venous whole blood was extracted from patients in a fasting state in the morning. After that, 5μL CD4FITC/CD8PE/CD3PerCP reagents were added into a flow tube. Besides, 20μL ethylenediaminetetraacetic acid (EDTA) for anticoagulation. Then, it was oscillated and mixed evenly before being placed away from light at room temperature for 15 minutes. Next, 450μL 10×disposable hemolysin was added and then kept away from light at room temperature for 15 minutes. After the samples were fully dissolved in the blood, FACSCalibur FCM was used to detect T-lymphocyte subpopulation levels. In addition, multiset software (BD Company, U.S.) was used for the analysis and measurement of CD4⁺ (normal range: 27% to 51%), CD8⁺ (normal range: 15% to 44%), and the ratio of CD4⁺ to CD8⁺ (normal range: 1.4 to 2.0).

Synthesis of mPEG-HA

EDC/NHS was used as amid condensation agent to modify HA with PEG. After that, 10mg HA, 25.65mg

0.13mmol EDC, and 15.40mg 0.13mmol NHS were weighed and then dissolved in phosphate buffer solution (PBS) with pH7.4. Next, the mixed solution was activated at room temperature for 2 hours. Besides, 5.36mg, 10.72mg, 16.08mg, and 21.44mg mPEG-NH₂ were weighed and then dripped into the reaction system. At room temperature, the reaction was continued for 24 hours. The reaction products were dialyzed with dialysis bags for 48 hours and then purified. After the products were frozen and dried, deuterated heavy water was used as the solvent. After that, the structure was characterized by MercuryPlus 400 nuclear magnetic resonance spectrometer and FTIR was utilized to measure its infrared absorption spectrum. Finally, the degree of substitution of mPEG on HA was calculated by the comparison of the integral areas of mPEG methylene in the nuclear magnetic resonance spectrum (-OCH₂CH₂-:δ=3.71 ppm) and methyl in HA (-COCH₃:δ=2.05 ppm).

Preparation of mPEG-HA-Pt

Firstly, 18.90mg, 0.05mM DACHPt and 16.99mg 0.1mM AgNO₃ were weighed and then suspended in deionized water under ultrasonic conditions. After that, the reaction lasted for 24 hours away from light to form a mixed solution of DACHPt. Then, the mixed solution was centrifuged at 3000rpm for 10 minutes to remove AgCl precipitate. After that, the remaining solution was filtered with 0.22μm millipore filter. A certain amount of mPEG-HA with different degrees of substitution was taken and then added into DACHPt mixed solution. The measurement result was [DACHPt]/[COOH]=1.0. The reaction products were stirred away from light for 120 hours. Next, ultra-filtration (MW 100KDa) was adopted to remove free DACHPt. Finally, DACHPt targeting nanomicelle (mPEG-HA-Pt) was successfully prepared.

Characterization of mPEG-HA-Pt

The mPEG-HA-Pt prepared above was performed with dynamic light scattering and Zeta potential detection. 1mL mPEG-HA-Pt and 1mL blank sample were taken for the detection of particle size and polydispersity with a Zetasizer Nano ZS90 nano-particle potentiometer. Next, a transmission electron microscope (TEM) was used to observe the size and morphology of mPEG-HA-Pt. In addition, inductively coupled plasma-mass spectrometry (ICP-MS) was adopted to measure the content of Pt in mPEG-HA-Pt.

Encapsulation efficiency referred to the ratio of DACHPt encapsulated in mPEG-HA-Pt to the total mass of the drug of DACHPt. Drug loading capacity referred to the percentage of DACHPt in mPEG-HA-Pt among total preparation. The calculation method for drug loading capacity was displayed in equation [3] below.

$$[3] \text{ Drug loading} = \text{Drug quality in micelles} / \text{Total mass of drug} \times 100\%$$

Statistical methods

The research data were processed and analyzed with SPSS19.0 statistical software. Measurement data were denoted by mean±standard deviation ($\bar{x} \pm s$) and enumeration data were expressed as a percentage (%). $P < 0.05$ indicated that the result showed statistical significance.

Results

Nuclear magnetic resonance spectrum analysis of mPEG-HA

The structure of mPEG-HA was confirmed by the nuclear magnetic resonance spectrum, as shown in Figure 1 below. According to Figure 1, (-COCH₃:δ=2.05 ppm) represented the integral area of methyl in HA and (-OCH₂CH₂-:δ=3.71 ppm) referred to the integral area of mPEGmethylene in HA in the nuclear magnetic resonance spectrum. The integral areas were compared to calculate the degree of substitution of mPEG on HA.

Measurement of mPEG-HA infrared spectrum

The analysis of mPEG-HA infrared spectrum was shown in Figure 2 below. It was demonstrated that the stretching vibration peak of C-O in the OHC-PEG-CHO group appeared at 2479.1 cm⁻¹, the stretching vibration peak of C-O in the Gal-PEG-CHO group was displayed at 2412.4cm⁻¹, and the stretching vibration peak of C-N was found at 1793.1cm⁻¹. The above results suggested that HA was successfully plugged into mPEG.

The particle size of mPEG-HA-Pt and Zeta potential

The detection results of particle size of mPEG-HA-Pt and Zeta potential were displayed in Figure 3 below. The particle size of mPEG-HA-Pt ranged between 78nm and 100nm with an average of 84.6±7.5nm. With the degree of substitution of PEG rose from 0% to 5%, mPEG-HA-Pt particle size gradually reduced, which indicated that mPEG-HA-Pt formed by PEG-modified HA became more stable.

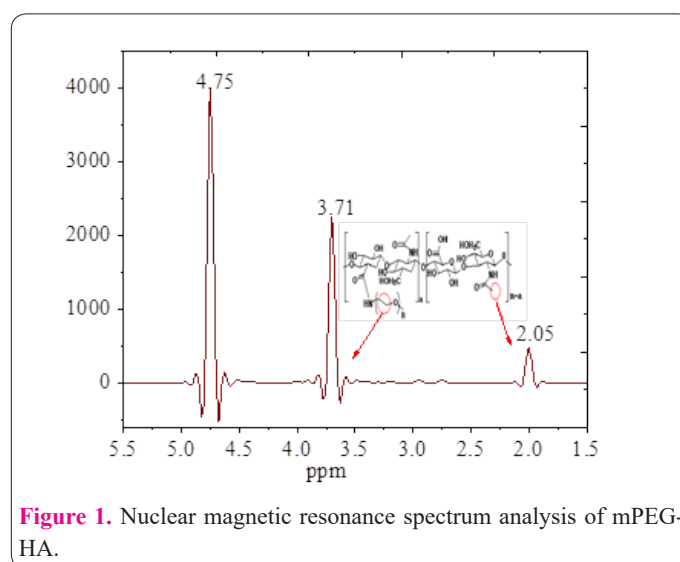


Figure 1. Nuclear magnetic resonance spectrum analysis of mPEG-HA.

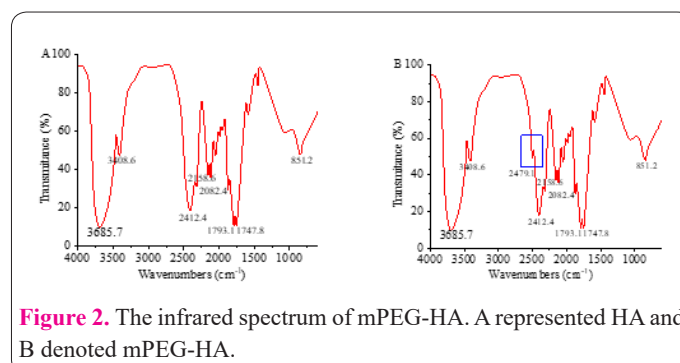


Figure 2. The infrared spectrum of mPEG-HA. A represented HA and B denoted mPEG-HA.

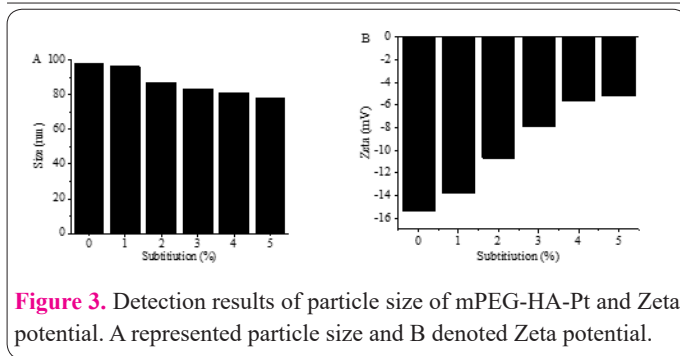


Figure 3. Detection results of particle size of mPEG-HA-Pt and Zeta potential. A represented particle size and B denoted Zeta potential.

Morphological characterization of mPEG-HA-Pt

A TEM was used to observe the morphology of mPEG-HA-Pt, as shown in Figure 4 below. Some spheres with uniform size (particle size less than 100nm) could be seen in Figure 4, which fully demonstrated that the synthetic product of mPEG-HA bound to DACHPt to form micelles with nucleocapsid structure.

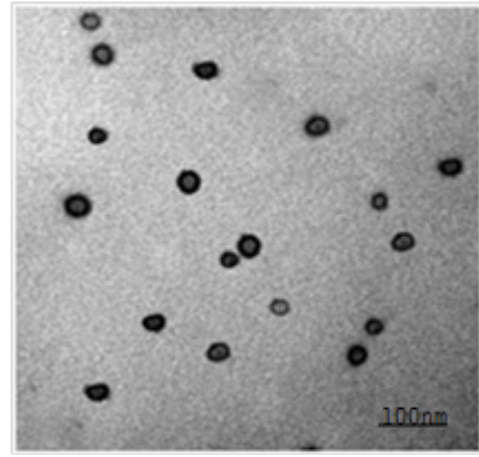


Figure 4. Electron microscopic image of mPEG-HA-Pt.

Measurement of drug loading capacity and encapsulation efficiency of mPEG-HA-Pt by ICP-MS

ICP-MS was employed to measure drug loading capacity and encapsulation efficiency of mPEG-HA-Pt, which were 18.7% and 87.4%, respectively. As the degree of substitution of PEG rose from 0% to 5%, both drug loading capacity and encapsulation efficiency showed a descending trend, which demonstrated that mPEG-HA-Pt became more stable with the modification of PEG, as illustrated in Figure 5 below.

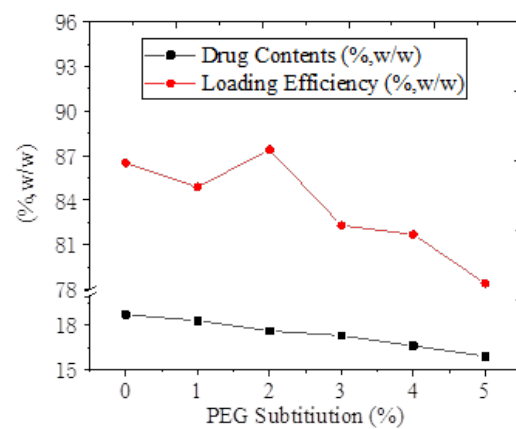


Figure 5. Measurement results of drug loading capacity and encapsulation efficiency of mPEG-HA-Pt.

Results of in vitro release test on mPEG-HA-Pt

The dialysis method was adopted to measure the results of in vitro release test on the drug DACHPt in mPEG-HA-Pt, as shown in Figure 6 below. It was found that DACHPt was released continuously from mPEG-HA-Pt. DACHPt release process mainly included two stages, including sudden release in the first 5 hours and continuous slow release after 15 hours. As the degree of substitution of PEG gradually rose from 0% to 1%, 2%, and 5%, the release rate of DACHPt gradually became slow, which suggested that PEG in outer layers might inhibit the occurrence of the exchange interaction between ions and reduce the release rate of DACHPt.

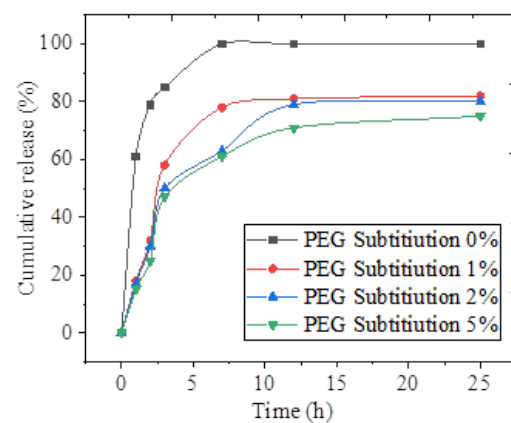


Figure 6. Results of in vitro release test on mPEG-HA-Pt.

Levels of CD4+ and CD8+ lymphocytes in the treatment group and control group

FCM was adopted to measure the expressions of CD4+ and CD8+ lymphocytes in the intervention group and the control group, as shown in Figure 7A. Compared with that in the control group, CD4+ lymphocyte level in the intervention group significantly increased, while CD8+ lymphocyte level apparently decreased. The differences were statistically significant ($P < 0.05$), as displayed in Figures 7B and 7C below.

Correlation between efficacy evaluation results and the changes in T-lymphocyte subpopulations

After 2 courses of treatment, the efficacy evaluation on 38 patients in the intervention group was carried out. It was found that there were 8 cases with PR (21.04%), 19 cases with SD (50.1%), 9 cases with PD (23.65%), and 2 cases with CR (5.21%). Besides, the rates of relative risk (RR) and community-based rehabilitation (CBR) reached 26.31% and 76.31%, respectively. After 2 courses

of chemotherapy, the expressions of CD4+ and the ratio of CD4+ to CD8+ among the patients with good efficacy evaluation remarkably improved, while the expression of CD8+ significantly decreased. The differences were all statistically significant ($P < 0.05$), as illustrated in Figure 8 below. The above results showed that there was a positive proportional relationship between the results of different efficacy evaluations and T-lymphocyte subpopulation levels among patients. A more significant therapeutic effect indicated the more significant rehabilitation of patients'

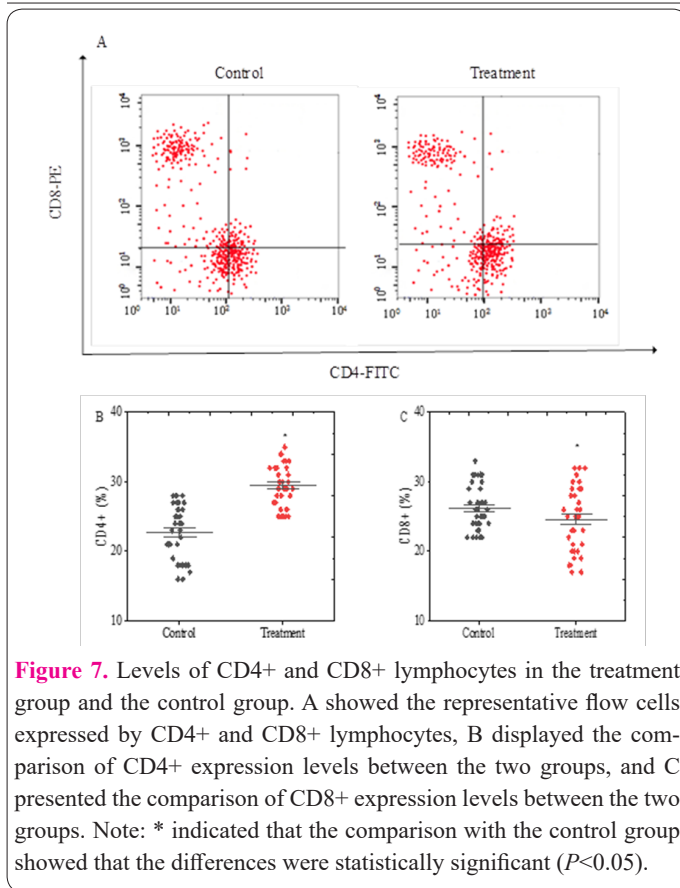


Figure 7. Levels of CD4+ and CD8+ lymphocytes in the treatment group and the control group. A showed the representative flow cells expressed by CD4+ and CD8+ lymphocytes, B displayed the comparison of CD4+ expression levels between the two groups, and C presented the comparison of CD8+ expression levels between the two groups. Note: * indicated that the comparison with the control group showed that the differences were statistically significant ($P < 0.05$).

immune functions.

Discussion

With the rapid development of molecular biology, humans gradually find that the occurrence, development, metastasis, and recurrence of malignant tumors are all related to the immune functional mechanism in the body, especially in cell immunity (16). T-lymphocyte and its subpopulations play an important role in the immune functional mechanism. The changes in T-lymphocyte subpopulation levels lead to the abnormality of body immune functions. T-lymphocyte includes multiple subpopulations with different immune functions. CD4+ lymphocyte plays a central role in the immune response. Its main function is the assistance and amplification of the production of antibodies and the activation of macrophages (17). CD8+ lymphocyte plays a role in the inhibition of immune response and activation. It directly inhibits the cytotoxic effect generated by antigen-presenting cells. Antigen-specific Th and B cells are the target cells, which secrete inhibiting factors to mediate effects (18).

mPEG is a non-toxic material that can form a good barrier on the surface of drugs to change the kinetic characteristics of targeted drugs and effectively reduce drug discharge rate. What's more, mPEG can protect HA biodegradation and increase the retention time of HA in the blood system to improve drug efficacy. DACHPt shows poor water solubility. Drug carriers can increase their water solubility to reach tumors and achieve targeted therapy (19-21). In this research, DACHPt was used to react with silver nitrate to form water PEG, which was distributed on the surface of nanomicelles. After that, it bound to mPEG-HA to form mPEG-HA-Pt by complexation reaction. Besides, film dispersion method was adopted to form

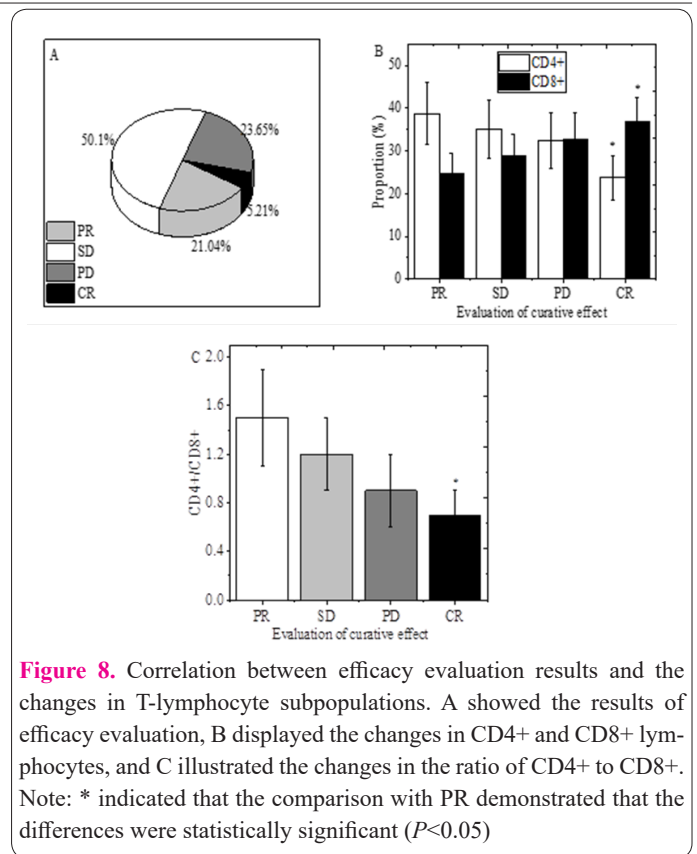


Figure 8. Correlation between efficacy evaluation results and the changes in T-lymphocyte subpopulations. A showed the results of efficacy evaluation, B displayed the changes in CD4+ and CD8+ lymphocytes, and C illustrated the changes in the ratio of CD4+ to CD8+. Note: * indicated that the comparison with PR demonstrated that the differences were statistically significant ($P < 0.05$).

nanomicelles and DACHPt was encapsulated in nucleus. The particle size of mPEG-HA-Pt nanomicelle ranged from 78nm to 100nm with an average of 84.6 ± 7.5 nm. Under TEM, spherical structures with uniform size could be observed. With the rise of the degree of substitution of PEG, drug loading capacity and encapsulation efficiency of drugs gradually reduced.

In recent years, the continuous exploration of relevant studies enables scholars to find that the occurrence and development of NSCLC are closely associated with the functions of immune cell subpopulations. In this research, abnormal immune function disorder among patients with NSCLC occurred. After 2 courses of nano drug treatment, patients' immune cell functions were significantly improved. The expressions of CD4+ and the ratio of CD4+ to CD8+ apparently enhanced, while the expression of CD8+ cells obviously decreased. The differences were statistically significant ($P < 0.05$). Dantoin et al (2021) (22) believed that nano drug loading therapy could obviously improve the immune functions of patients with middle and advanced NSCLC.

To further the relationship between the therapeutic effects on patients with NSCLC and immune cell functions, patients' cell immune functions were remarkably improved after 2 courses of treatment. The improvement of cell immune functions among patients with PR as efficacy evaluation result was more significant than that among patients with SD and PD as efficacy evaluation results, which was similar to the research outcome obtained by Zhai et al (2020) (23). The above research results demonstrated that a more significant therapeutic effect indicated better rehabilitation of patients' immune functions, which might result from the effective control of tumor proliferation, progression, and metastasis among NSCLC patients with good therapeutic effects.

In the research, a kind of targeting nanomicelle system

(mPEG-HA-Pt) formed by HA and DACHPt modified by mPEG was designed to increase the high-level concentration of drugs at tumor sites among NSCLC patients. After nanomicelle therapy for NSCLC patients, their cell immune functions were all improved, especially among the patients with good efficacy evaluation. The disadvantages of this research lie in the stability of mPEG-HA-Pt nanomicelle system needs to be further optimized despite successful preparation. Besides, the sample size is limited. In follow-up studies, the sample size should be enlarged to further investigate whether the improvement of patients' cell immune functions can help improve the therapeutic effect of chemotherapy. In conclusion, the research provided reference and basis for the implementation of timely and reasonable immunotherapy among NSCLC patients.

Acknowledgments

Not applicable.

Interest conflict

The authors declare that they have no conflict of interest.

Fundings

The research is supported by: This work was supported by the General scientific research project of Zhejiang Provincial Department of Education(Y201636648) and the Ningbo natural fund project(2018A610277).

References

- Pennell NA, Arcila ME, Gandara DR, West H. Biomarker Testing for Patients With Advanced Non-Small Cell Lung Cancer: Real-World Issues and Tough Choices. *Am Soc Clin Oncol Educ Book*. 2019 Jan;39:531-542. doi: 10.1200/EDBK_237863. Epub 2019 May 17. PMID: 31099633.
- Nagano T, Tachihara M, Nishimura Y. Molecular Mechanisms and Targeted Therapies Including Immunotherapy for Non-Small Cell Lung Cancer. *Curr Cancer Drug Targets*. 2019;19(8):595-630. doi: 10.2174/1568009619666181210114559. PMID: 30526458.
- Adderley H, Blackhall FH, Lindsay CR. KRAS-mutant non-small cell lung cancer: Converging small molecules and immune checkpoint inhibition. *EBioMedicine*. 2019 Mar;41:711-716. doi: 10.1016/j.ebiom.2019.02.049. Epub 2019 Mar 7. PMID: 30852159; PMCID: PMC6444074.
- Ostroumov D, Fekete-Drimusz N, Saborowski M, Kühnel F, Woller N. CD4 and CD8 T lymphocyte interplay in controlling tumor growth. *Cell Mol Life Sci*. 2018 Feb;75(4):689-713. doi: 10.1007/s00018-017-2686-7. Epub 2017 Oct 14. PMID: 29032503; PMCID: PMC5769828.
- Zander R, Schauder D, Xin G, Nguyen C, Wu X, Zajac A, Cui W. CD4⁺ T Cell Help Is Required for the Formation of a Cytolytic CD8⁺ T Cell Subset that Protects against Chronic Infection and Cancer. *Immunity*. 2019 Dec 17;51(6):1028-1042.e4. doi: 10.1016/j.immuni.2019.10.009. Epub 2019 Dec 3. PMID: 31810883; PMCID: PMC6929322.
- Hirahara K, Kokubo K, Aoki A, Kiuchi M, Nakayama T. The Role of CD4⁺ Resident Memory T Cells in Local Immunity in the Mucosal Tissue - Protection Versus Pathology. *Front Immunol*. 2021 Apr 21;12:616309. doi: 10.3389/fimmu.2021.616309. PMID: 33968018; PMCID: PMC8097179.
- Rossi D, Dannhauser D, Telesco M, Netti PA, Causa F. CD4⁺ versus CD8⁺ T-lymphocyte identification in an integrated microfluidic chip using light scattering and machine learning. *Lab Chip*. 2019 Nov 21;19(22):3888-3898. doi: 10.1039/c9lc00695h. Epub 2019 Oct 23. PMID: 31641710.
- Perugino CA, Kaneko N, Maehara T, Mattoo H, Kers J, Allard-Chamard H, Mahajan VS, Liu H, Della-Torre E, Murphy SJH, Ghebremichael M, Wallace ZS, Bolster MB, Harvey LM, Mylvaganam G, Tuncay Y, Liang L, Montesi SB, Zhang X, Tinju A, Mochizuki K, Munemura R, Sakamoto M, Moriyama M, Nakamura S, Yosef N, Stone JH, Pillai S. CD4⁺ and CD8⁺ cytotoxic T lymphocytes may induce mesenchymal cell apoptosis in IgG₄-related disease. *J Allergy Clin Immunol*. 2021 Jan;147(1):368-382. doi: 10.1016/j.jaci.2020.05.022. Epub 2020 May 30. PMID: 32485263; PMCID: PMC7704943.
- Zander R, Kasmani MY, Chen Y, Topchyan P, Shen J, Zheng S, Burns R, Ingram J, Cui C, Joshi N, Craft J, Zajac A, Cui W. Tfh-cell-derived interleukin 21 sustains effector CD8⁺ T cell responses during chronic viral infection. *Immunity*. 2022 Mar 8;55(3):475-493.e5. doi: 10.1016/j.immuni.2022.01.018. Epub 2022 Feb 24. PMID: 35216666; PMCID: PMC8916994.
- Choi SM, Park HJ, Choi EA, Jung KC, Lee JI. Cellular heterogeneity of circulating CD4⁺CD8⁺ double-positive T cells characterized by single-cell RNA sequencing. *Sci Rep*. 2021 Dec 8;11(1):23607. doi: 10.1038/s41598-021-03013-4. PMID: 34880348; PMCID: PMC8655006.
- Xue Y, Gao S, Gou J, Yin T, He H, Wang Y, Zhang Y, Tang X, Wu R. Platinum-based chemotherapy in combination with PD-1/PD-L1 inhibitors: preclinical and clinical studies and mechanism of action. *Expert Opin Drug Deliv*. 2021 Feb;18(2):187-203. doi: 10.1080/17425247.2021.1825376. Epub 2020 Oct 5. PMID: 32954856.
- Wang S, Gou J, Wang Y, Tan X, Zhao L, Jin X, Tang X. Synergistic Antitumor Efficacy Mediated by Liposomal Co-Delivery of Polymeric Micelles of Vinorelbine and Cisplatin in Non-Small Cell Lung Cancer. *Int J Nanomedicine*. 2021 Mar 22;16:2357-2372. doi: 10.2147/IJN.S290263. PMID: 33790554; PMCID: PMC7997865.
- Gong F, Wang R, Zhu Z, Duan J, Teng X, Cui ZK. Drug-interactive mPEG-*b*-PLA-Phe(Boc) micelles enhance the tolerance and anti-tumor efficacy of docetaxel. *Drug Deliv*. 2020 Dec;27(1):238-247. doi: 10.1080/10717544.2020.1718245. PMID: 32003299; PMCID: PMC7034090.
- Chen L, Wang S, Liu Q, Zhang Z, Lin S, Zheng Q, Cheng M, Li Y, Cheng C. Reduction sensitive nanocarriers mPEG-g-γ-PGA/SSBPEI@siRNA for effective targeted delivery of survivin siRNA against NSCLC. *Colloids Surf B Biointerfaces*. 2020 Sep;193:111105. doi: 10.1016/j.colsurfb.2020.111105. Epub 2020 May 5. PMID: 32417465.
- Velez EM, Desai B, Ji L, Quinn DI, Colletti PM, Jadvar H. Comparative prognostic implication of treatment response assessments in mCRPC: PERCIST 1.0, RECIST 1.1, and PSA response criteria. *Theranostics*. 2020 Feb 10;10(7):3254-3262. doi: 10.7150/thno.39838. PMID: 32194866; PMCID: PMC7053201.
- Preglej T, Hamminger P, Luu M, Bulat T, Andersen L, Göschl L, Stolz V, Rica R, Sandner L, Waltenberger D, Tschismarov R, Faux T, Boenke T, Laiho A, Elo LL, Sakaguchi S, Steiner G, Decker T, Bohle B, Visekruna A, Bock C, Strobl B, Seiser C, Boucheron N, Ellmeier W. Histone deacetylases 1 and 2 restrain CD4⁺ cytotoxic T lymphocyte differentiation. *JCI Insight*. 2020 Feb 27;5(4):e133393. doi: 10.1172/jci.insight.133393. PMID: 32102981; PMCID: PMC7101144.
- Wang Q, Li S, Qiao S, Zheng Z, Duan X, Zhu X. Changes in T Lymphocyte Subsets in Different Tumors Before and After Radiotherapy: A Meta-analysis. *Front Immunol*. 2021 Jun 16;12:648652. doi: 10.3389/fimmu.2021.648652. PMID: 34220806; PMCID: PMC8242248.

18. Imai N, Tawara I, Yamane M, Muraoka D, Shiku H, Ikeda H. CD4⁺ T cells support polyfunctionality of cytotoxic CD8⁺ T cells with memory potential in immunological control of tumor. *Cancer Sci.* 2020 Jun;111(6):1958-1968. doi: 10.1111/cas.14420. Epub 2020 May 12. PMID: 32304127; PMCID: PMC7293103.
19. Shi M, Wang Y, Zhao X, Zhang J, Hu H, Qiao M, Zhao X, Chen D. Stimuli-Responsive and Highly Penetrable Nanoparticles as a Multifunctional Nanoplatfrom for Boosting Nonsmall Cell Lung Cancer siRNA Therapy. *ACS Biomater Sci Eng.* 2021 Jul 12;7(7):3141-3155. doi: 10.1021/acsbomaterials.1c00582. Epub 2021 Jun 17. PMID: 34137580.
20. Lin Y, Zhuang X, Xie B, Chen H. Enhanced Antitumor Efficacy of Docetaxel-Loaded Monomethoxy Poly(ethylene glycol)-Poly(D, L-lactide-co-glycolide) Amphiphilic Copolymer Against Non-Small Cell Lung Cancer. *J NanosciNanotechnol.* 2020 Dec 1;20(12):7263-7270. doi: 10.1166/jnn.2020.18756. PMID: 32711589.
21. Wu W, Wu J, Fu Q, Jin C, Guo F, Yan Q, Yang Q, Wu D, Yang Y, Yang G. Elaboration and characterization of curcumin-loaded Tri-CL-mPEG three-arm copolymeric nanoparticles by a micro-channel technology. *Int J Nanomedicine.* 2019 Jul 2;14:4683-4695. doi: 10.2147/IJN.S198217. PMID: 31308653; PMCID: PMC6615023.
22. Dantoing E, Piton N, Salaün M, Thiberville L, Guisier F. Anti-PD1/PD-L1 Immunotherapy for Non-Small Cell Lung Cancer with Actionable Oncogenic Driver Mutations. *Int J Mol Sci.* 2021 Jun 11;22(12):6288. doi: 10.3390/ijms22126288. PMID: 34208111; PMCID: PMC8230861.
23. Zhai X, Zhang J, Tian Y, Li J, Jing W, Guo H, Zhu H. The mechanism and risk factors for immune checkpoint inhibitor pneumonitis in non-small cell lung cancer patients. *Cancer Biol Med.* 2020 Aug 15;17(3):599-611. doi: 10.20892/j.issn.2095-3941.2020.0102. PMID: 32944393; PMCID: PMC7476083.